January 2013

Mechanical properties of human amniotic fluid stem cells using nanoindentation

Ashkan Aryaei
University of Toledo

Ambalangodage Jayasuriya
University of Toledo

Recommended Citation

Ashkan Aryaei and Ambalangodage Jayasuriya. "Mechanical properties of human amniotic fluid stem cells using nanoindentation" *Journal of Biomechanics* (2013): 1524-1530. https://doi.org/10.1016/j.jbiomech.2013.03.023

HHS Public Access

Author manuscript

J Biomech. Author manuscript; available in PMC 2016 July 01.

Published in final edited form as:

J Biomech. 2013 May 31; 46(9): 1524–1530. doi:10.1016/j.jbiomech.2013.03.023.

Mechanical properties of human amniotic fluid stem cells using nanoindentation

Ashkan Aryaei[a] and **Ambalangodage C. Jayasuriya**[b,*]

[a]Department of Mechanical Engineering, University of Toledo, 1650 N. Westwood Avenue, Toledo, OH 43606-3390, USA

[b]Department of Orthopaedic Surgery, University of Toledo, MS 1094, 3065 Arlington Avenue, Toledo, OH 43614-5807, USA

Abstract

The aim of this study was to obtain nanomechanical properties of living cells focusing on human amniotic fluid stem (hAFS) cell using nanoindentation techniques. We modified the conventional method of atomic force microscopy (AFM) in aqueous environment for cell imaging and indentation to avoid inherent difficulties. Moreover, we determined the elastic modulus of murine osteoblast (OB6) cells and hAFS cells at the nucleus and cytoskeleton using force–displacement curves and Hertz theory. Since OB6 cell line has been widely used, it was selected to validate and compare the obtained results with the previous research studies. As a result, we were able to capture high resolution images through utilization of the tapping mode without adding protein or using flxation methods. The maximum depth of indentation was kept below 15% of the cell thickness to minimize the effect of substrate hardness. Nanostructural details on the surface of cells were visualized by AFM and fluorescence microscopy. The cytoskeletal fibers presented remarkable increase in elastic modulus as compared with the nucleus. Furthermore, our results showed that the elastic modulus of hAFS cell edge (31.6 kPa) was lower than that of OB6 cell edge (42.2 kPa). In addition, the elastic modulus of nucleus was 13.9 kPa for hAFS cell and 26.9 kPa for OB6 cells. Differences in cell elastic modulus possibly resulted from the type and number of actin cytoskeleton organization in these two cell types.

Keywords

Atomic force microscopy; Osteoblast; Human amniotic fluid stem cells; Nanoindentation; Elastic modulus

1. Introduction

Finding mechanical properties of biological samples, especially living cells, has been of great interest to researchers. Analysis of cellular mechanical properties can lead us to discover new methods of identifying various forms of cancers (Brandão et al., 2003; Cross et

*Corresponding author. Tel.: +1 419 383 6557; fax: +1 419 383 3526. a.jayasuriya@utoledo.edu (A.C. Jayasuriya).

Conflict of interest statement

We declare that none of the authors involved in this research work have conflict of interest.

al., 2007; Lekka, 2012) and other diseases (Suresh, 2006). In tissue engineering, probing the elasticity and adhesion of live cells can provide physical insight into the mechanical and chemical properties of biomaterials and scaffold materials (Simon et al., 2004). Many methods including magnetic twisting cytometry, traction force microscopy, micro-pipette aspiration, optical trap, optical stretcher, micro- and nano-needle insertion and atomic force microscopy (AFM) have been used to find the mechanical properties of cells (Bao and Suresh, 2003; Lim et al., 2006). Compared to the other methods, AFM indentation has become the principal technique in measuring the cell mechanical properties of surface layers and especially cells with high spatial precision (Casuso et al., 2011; Quist and Lal, 2012). Although there are some limitations in using AFM for the measurement of cell mechanics such as lateral drag of the cell by the tip, the calibration (Kirmizis and Logothetidis, 2010) and not ideally sharp probes (Wu et al., 2012), this method is the most widely used.

The elastic modulus of a living cell is usually calculated by producing force–displacement curves with data from indentation tests. The common analysis models for cell indentation are based on the Hertz theory (Hertz, 1882; Sneddon, 1965). This model is based on perfectly elastic behavior of cells during indentation (Weisenhorn et al., 1993). In the application to the AFM measurements the generally considered indenter's geometries are the conical and spherical ones. Although nanoindentation is widely used to investigate the stem cell mechanical properties (Darling et al., 2008), these properties for some new types of stem cells have not yet been fully discovered.

In last few decades, main advancement has been facilitated by the discovery of stem cells, capable of converting to various cell lineages. Stem cells have been isolated from embryonic, fetal, and adult tissues and more recently, also from umbilical cord, placenta and amniotic fluid. Among the source of stem cells that have been studied, human Amniotic Fluid Stem (hAFS) cells have arisen as an attractive source of stem cells since 2007 (Siegel et al., 2008), as its procurement does not raise the ethical concerns associated with the use of human embryonic stem cells (Rodrigues et al., 2012a, 2012b; Siegel et al., 2007). In addition, hAFS cells have the advantage of being primitive cells with little known antigenicity and great expansion capabilities. These cells can be induced to differentiate into cells that represent each germ layer, such as adipogenic, osteogenic, myogenic, endothelial, neuronal, hepatic, and chondrogenic lineages (Cananzi et al., 2009; Joo et al., 2012). hAFS cells are becoming an important source of cells for regenerative medicine and tissue engineering. In this way, it is necessary to characterize its mechanical properties. In other words, although hAFS cells have many properties that support their clinical usefulness (Skardal et al., 2012), little is known about the mechanical properties.

In this study, the aim was to determine the mechanical properties of hAFS cells and compare them to murine osteoblast (OB6) cells as a reference using AFM imaging and indentation with the Hertz model. Specifically, we chose OB6 cells as a reference cell source since our laboratory focuses on OBs for the bone regeneration studies. The OB6 cells are well known cells with the previously known mechanical properties (Charras and Horton, 2002; Darling et al., 2008) to verify the result of current technique and discuss the possible source of differences with other papers. Both nucleus and cytoskeleton play an important role in cell deformation and mechanical properties. Thus, indentation was done at nucleus and

cytoskeleton regions of the cells. The tapping mode was used for cell imaging in physiological aqueous environment without using fluid cell or any other specific equipments. In addition, this physiological aqueous environment provided the advantage of tapping mode without requiring adhesive proteins to attach cells on the substrate. In addition, images obtained from AFM were compared with fluorescence microscopy images to verify the viability of cells used for AFM studies. Generally, there were two aims in this paper. First, a new and simple technique of imaging and indenting for living cells in tapping mode was introduced. Secondly, the elastic modulus for hAFS cells, as an attractive new stem cell source, was determined using the above technique and validated using OB6 cells.

2. Materials and methods

2.1. Materials

The hAFS cells (passage 21) were kindly provided by Wake Forest Institute for Regenerative Medicine (Winston-Salem, NC, USA). Chang media containing alpha minimum essential medium (α-MEM) (GIBCO), 18% Chang Medium B (Irvine Scientific), 2% Chang Medium C (Irvine Scientific), 15% Fetal Bovine Serum (FBS) (GIBCO), and 1% Pen Strep (GIBCO) were used to prepare cell culture medium. OB6 cell vials were received from Dr. Lecka Czernik at the University of Toledo. α-MEM supplemented with 10% FBS and 1% penicillin–streptomycin was used to culture the cells. A LIVE/DEAD cell assay kit (Invitrogen) was used to identify cell viability and morphology. To prepare AFM samples, microscope slides with 1 mm thickness (Fisher Scientific) were used.

For consistency, we applied the same preparation procedures for both types of cells. Small pieces of microscope slides (1 cm × 1 cm) were cleaned with ethyl alcohol and deionized water and kept under UV light for 90 min. Approximately 10,000 cells were counted by a hemocytometer after trypsinization from the original plate and plated into 35 mm petri dish filled with small pieces of sterilized microscope slides. The petri dish was incubated (37 °C, 5% CO_2) for 36 h before experiment.

2.2. Instruments

AFM indentation testing and imaging were performed with a commercial instrument Veeco Multimode with nanoscope V Controller with J scanner. The maximum Z range for this scanner was about 6 μm which is usually higher than the maximum height of cells (Charm et al., 2002; Costa, 2006; Fung et al., 2010). The NanoScope software V6.13 was used to control imaging and testing parameters. In this experiment, cantilevers B and D from probe SNL-10 (Bruker Co.) were used with a spring constant of 0.12 N/m and 0.06 N/m, respectively. The tip half opening angle was assumed to be 25° from the specifications of the manufacturer. This sharpened probe is suitable for performing experiments in both air and fluid while applied load is in a range of a few nanonewtons for better resolution (Vié et al., 2000; Wu et al., 2012). Fluorescence microscopy (Olympus, FSX100) was used to obtain cell images when cells were treated as the LIVE/DEAD cell as previously described in detail (Jayasuriya and Bhat, 2010). Data were statistically analyzed with one-way ANOVA. $p<0.05$ was considered as statistically significant.

2.3. AFM imaging and indentation test

To perform the AFM test, a small piece of microscope slide covered by cells was attached to a conductive metal plate on top of the AFM scanner. In order to minimize the viscosity effects, low scanning speed of 1 Hz was used for imaging (Costa et al., 2006; Rotsch and Radmacher, 2000). By indenting slowly enough, the viscous contributions will be very small (Zhu et al., 2011). Then, the force measurements will only be demonstrated by the elastic behavior of cell. In the first series of experiments, we tried to apply AFM contact mode in air and fluid using fluid cell to obtain better resolution. However, due to the lack of strong adhesion between cells and microscope slides, the cells were detached and the test could not be conducted completely as expected (Simon and Durrieu, 2006). Furthermore, air bubbles were a problem as they sit on the cantilever when fluid cell is used as expected from literature (Jena and Hörber, 2002). Fig. 1 shows an image captured in air using the contact mode. After some tip tracing–retracing movement, cells were detached from the glass substrate due to the low adhesion forces.

In the next step, as schematically shown in Fig. 2, the culture medium was injected on the cell surface by using a small syringe needle. A drop of culture medium covered the entire cell and cantilever. By applying this modified technique, cells were attached to the glass due to the adhesion force between the small drops of the culture medium and glass surface. Cell attachment to the surface is vital for cell survival and growth (Basson et al., 1992; Bourdoulous et al., 1998). Therefore, all parts of the experiment were completed within 1–2 h before cells started to die and detach from the small pieces of the glass slides (Allison et al., 2010; Favre et al., 2011; Simon et al., 2003). By using a force mode modulus, an indentation with low applied loads was done on the surface of the cell to obtain its elastic modulus with the Hertz model. The AFM indentation experiment required monitoring the deflection of the cantilever probe as it indents the cell surface. The resulting interaction force bends the cantilever, which is detected by the motion of laser spot reflected off the back of cantilever onto a four-quadrant photodetector. For each kind of cell, the indentation test was done at least 20 times. Before plotting a force indentation curve, the sensitivity of the AFM cantilever should be calculated. Thus, we indented a glass substrate using the same tip. Glass is comparatively hard enough to be considered as a rigid substrate.

2.4. Analysis of data

A simple model of quantifiying the elastic response of materials is based on the Hertz model which has been frequently used in previous cell study studies (Chen et al., 2010; Kelly et al., 2011; Titushkin and Cho, 2007). The Hertz model predicts elastic modulus of the sample with the assumption of perfect elastic behavior and indenter shape of a rigid sphere or cone. Regarding the conical shape of the tip used in this set of experiments, the equation relating force and depth for indentation with a cone is given by

$$F=\frac{2}{\pi}tg\alpha\frac{E}{1-\upsilon^2}\delta^2 \quad (1)$$

In this equation, F is the load exerted by AFM tip, E is Young's modulus of the cell, α is the half opening angle of cantilever tip and υ is Poisson's ratio. Usually, $\upsilon = 0.5$ is assumed for cells and other perfect elastic materials (Costa, 2003). Thus, cells are considered as an incompressible material.

3. Results and discussion

3.1. Cell imaging and characterization

Fig. 3 shows fluorescence microscopy images of hAFS and OB6 cells. Live and healthy cells were stained as green. Investigation of the hAFS cell morphology showed distinct regions. hAFS cells were well-elongated in one direction as expected (Kim et al., 2007; Kolambkar et al., 2010) and the length of cells were normally longer than 200 μm. hAFS cell area was significantly larger compared with OB6 cell. Microtubules and filamentous structures spread out over hundreds of micrometers prevented the capture of the image of a whole hAFS cell because the maximum length that can be covered by AFM scanner was 100 μm (Fig. 4A). In addition, the cell nucleus has been identified with an asterisk (*) in this figure. Fig. 4B demonstrates the height distribution of the cell along a line that is shown in Fig. 4A. By comparing the height profile of two cells (a and b) shown in Fig. 4A, it was clear that by increasing the distance from the nucleus, the cytoskeletal height of the cell decreases. Detailed cytoskeletal fiber height is shown in the sub-figure of Fig. 4B. These cytoskeletal filaments play an important role in measuring the mechanical properties of cells (Costa, 2006). There were less than 10 filaments in a certain direction. According to this graph the approximate fiber height was around 50 nm. Generally, the nucleus portion of the cell constitutes its highest part (Haga et al., 2000). The approximate height of the hAFS cell nucleus was between 1 μm and 2.7 μm obtained by AFM.

Two elongated hAFS cells are shown in Fig. 4C obtained from AFM. Actin filaments and nucleus are visible in this figure. Thin and long actin filaments were also separately formed as indicated by arrows in this figure. In Fig. 4D, the three-dimensional image of Fig. 4C is presented. The average height for the nuclei was estimated around 1.3 μm for this cell which was the maximum thickness and height in the cell. In addition, the morphology of cells obtained with AFM imaging was consistent with fluorescence microscopy images asserting that cells were alive during the AFM test and the morphology has not been changed.

In tapping mode, taking good images is usually more difficult than in contact mode (Goldsbury et al., 2001). Although no external adhesive proteins or flxation methods were used to adhere cells to the glass, cells did not detach through AFM tapping mode. This was due to the injection of culture medium during the experiment. In this method, cell and tip were occupied by the big drop of cell culture medium which reduced the effect of capillary forces (Zitzler et al., 2002). The same method was applied for OB6 cells. Fig. 5 demonstrates the cytoskeleton height of OB6 cells in two paths within the same cell. Path 1 was selected closer to the cell nucleus compared with path 2. The average cell height in this path was larger than path 2 which means that as we get closer to the cell nucleus, the cell height increases and nucleus part was the highest cell part in both kinds of cell. The height of OB6 nucleus varied from 1.5 μm to 3.5 μm. OB6 cells had more actin filaments than hAFS cells. For OB6 cells, filaments had less height compared to hAFS cells and were more

scattered. In other words, the filaments of one OB6 cell were distributed over approximately 25 nm while in hAFS cells the cell filaments were distributed over 10 nm. The data obtained in this part are in agreement with Simon et al. (2003, 2004) papers, despite the fact that they used human bone marrow stromal cells.

3.2. Cell mechanical properties

Cells are soft and considered as the elastic materials under small loads and AFM indentation of live cells does not present evidence of cell plastic deformations. This is the main reason that usually very low force (~nN) is applied to the cell surface in order to obtain elastic modulus. A concern during the cell indentation experiment is to minimize the effect of glass substrate on force–displacement curves. To compensate for this, it is attempted to keep indentation depths equal to or less than 15% of the cell height (Jung et al., 2004; Mathur et al., 2001). In addition, we performed indentation tests at the nucleus and cytoskeleton of cells. Based on our findings, at the nucleus, cells were thicker than in the other parts. Another property of engaging indentation upon the nucleus is that the cytoskeletal structure is more homogeneous than the other parts of cell (Sirghi et al., 2008). Fig. 6A shows a schematic force–indentation curve of the nanoindentation experiment. As expected from the literature (Agnihotri and Siedlecki, 2005; Sen et al., 2005), adhesion jump occurred in both kinds of cells due to the adhesion. For hAFS cells this jump is higher than for OB6 cells.

Furthermore, Fig. 6B and C demonstrates a typical force–indentation curve for hAFS and OB6 cell nucleus indentation, respectively. At almost similar loads, indentation depth for hAFS cells was greater than for OB6 cells (approximately 1.6 times) and led to the lower elastic modulus based on the Hertz equation. Loading–unloading curves almost overlaped. This observation is in agreement with previous studies (Charras et al., 2001; Chen et al., 2010; Favre et al., 2011; Svaldo Lanero et al., 2006).

All applied forces were between 0.6 nN and 0.9 nN depending on the cantilever used. The narrow load range is due to the small changes in sensitivity and spring constant of the AFM tip during the indentation test and the two different tip spring constants. Comparison between elastic modulus of hAFS cells at nucleus and cytoskeleton revealed Young's modulus at edges consisting of actin filaments and microtubes were almost double the nucleus. It has been well established that the actin fibers promote overall cellular elasticity (Kagiwada et al., 2010; Sirghi et al., 2008).

Final results of elastic modulus are shown in Fig. 7. Cell population properties were well described by log-normal and Gaussian distributions. Both functions predicted approximately same value for elastic modulus of each case. Based on Gaussian fit, average elastic modulus of hAFS cells was 32.9±3.66 kPa at the cytoskeleton region and 13.9±2.25 kPa at the cell nucleus. Additionally, the average elastic modulus of OB6 was 26.9±3.41 kPa at nucleus region and 42.8±3.44 kPa for cytoskeleton. These values were in the range of elastic modulus previously reported for cells (Bao and Suresh, 2003). Based on the presented results, significant difference ($p<0.05$) was observed in the elastic modulus of nucleus and cytoskeleton for both kinds of cells.

Although some papers reported the same range values of elastic modulus for cells (Collinsworth et al., 2002; Yourek et al., 2007), some of the previously published investigations showed significantly lower elastic modulus (Darling et al., 2006, 2008; Takai et al., 2005). For instance, the average reported value for murine osteoblast cells is 14 kPa at cell nucleus (Charras and Horton, 2002) which shows a significant difference from the present results. This discrepancy reflects intrinsic differences among both cell lines and experimental setup. The main reason can be attributed to variations in methodology. For instance, the spring constant of the cantilever and the applied force (Aryaei et al., 2012; Qian et al., 2005) impress the obtained Young's modulus value. Furthermore, the method of testing has remarkable effects (Ruiz et al., 2012).

It has been demonstrated that (Nikkhah et al., 2011) culture conditions has a great influence on elastic properties of cells and composition of the growth medium can activate or deactivate certain proteins which subsequently promote focal adhesions and actin stress fiber formation that affect the overall cell elasticity. Moreover, it has been shown that stress relaxation (i.e. viscoelastic properties) of cells before AFM indentation has a great effect on the elastic modulus and a modified Hertz model (thin-layer model) is applied to describe the behavior (Darling et al., 2007).

The other factors are the indentation depth (Lekka et al., 2012; Pogoda et al., 2012) and AFM tip size/shape (Ng et al., 2007). Elastic modulus obtained based on small indentation depths is described as the regions rich in actin filaments while for large indentation depths, the modulus represents the stiffness of a whole cell which is usually lower than actin filaments network. In addition, using different shape and size of AFM tips has a significant effect on elastic modulus. Using sharper AFM tip in this study would be another source of difference with some other published results. Nanosized tips can sense actin filaments, mitochondrion and microtubules leading to higher elastic modulus of the cells. On the other hand microsized tips can contact the bigger area in many parts of cells. The measured elastic modulus is the average of the different parts of the cells.

4. Conclusion

The goal of this article was to find the elastic modulus of hAFS cells as a novel source of stem cells and compare its mechanical properties and cell morphology with OB6 cells as one of the widely used cell lineages. In addition, we presented a new method for cell imaging and indentation in an aqueous environment. In the new method, we tried to eliminate the inherent concerns of the current method of cell imaging and indentation. Our results displayed that hAFS cells were well elongated cells at the selected timepoint and their nucleus heights are lower than those of OB6 cells. Moreover, OB6 cells demonstrated higher number of filaments compared with hAFS cells.

Using the Hertz model, the elastic modulus of hAFS cells was reported to be double at the cytoskeleton part compared with the nucleus region. Furthermore, the highest elastic modulus was obtained for OB6 cytoskeleton and the lowest one was for hAFS cell nucleus. However, there are several parameters than can affect the elastic modulus values and further investigations need to be done to verify the current results.

Acknowledgments

This work was supported by the National Science Foundation (NSF) Grant #0652024 and the National Institute of Health (NIH) Grant #DE019508.

References

Agnihotri A, Siedlecki CA. Adhesion mode atomic force microscopy study of dual component protein films. Ultramicroscopy. 2005; 102:257–268. [PubMed: 15694672]

Allison DP, Mortensen NP, Sullivan CJ, Doktycz MJ. Atomic force microscopy of biological samples. Wiley Interdisciplinary Reviews: Nanomedicine and Nanobiotechnology. 2010; 2:618–634. [PubMed: 20672388]

Aryaei A, Jayatissa AH, Jayasuriya AC. Nano and micro mechanical properties of uncross-linked and cross-linked chitosan films. Journal of the Mechanical Behavior of Biomedical Materials. 2012; 5:82–89. [PubMed: 22100082]

Bao G, Suresh S. Cell and molecular mechanics of biological materials. Nature Materials. 2003; 2:715–725. [PubMed: 14593396]

Basson CT, Kocher O, Basson MD, Asis A, Madri JA. Differential modulation of vascular cell integrin and extracellular matrix expression in vitro by TGF-B1 correlates with reciprocal effects on cell migration+ Journal of Cellular Physiology. 1992; 153:118–128. [PubMed: 1522126]

Bourdoulous S, Orend G, MacKenna DA, Pasqualini R, Ruoslahti E. Fibronectin matrix regulates activation of RHO and CDC42 GTPases and cell cycle progression. The Journal of Cell Biology. 1998; 143:267–276. [PubMed: 9763437]

Brandão MM, Fontes A, Barjas-Castro ML, Barbosa LC, Costa FF, Cesar CL, Saad STO. Optical tweezers for measuring red blood cell elasticity: application to the study of drug response in sickle cell disease. European Journal of Haematology. 2003; 70:207–211. [PubMed: 12656742]

Cananzi M, Atala A, De Coppi P. Stem cells derived from amniotic fluid: new potentials in regenerative medicine. Reproductive Biomedicine Online. 2009; 18:17–27. [PubMed: 19281660]

Casuso I, Rico F, Scheuring S. Biological AFM: where we come from—where we are—where we may go. Journal of Molecular Recognition. 2011; 24:406–413. [PubMed: 21504017]

Charm, G.; Lehenkari, P.; Horton, M. Biotechnological applications of atomic force microscopy. In: Bhanu, P.; Jena, HJKH., editors. Methods in Cell Biology. Vol. Chapter 8. Academic Press; 2002. p. 171-191.

Charras GT, Horton MA. Determination of cellular strains by combined atomic force microscopy and finite element modeling. Biophysical Journal. 2002; 83:858–879. [PubMed: 12124270]

Charras GT, Lehenkari PP, Horton MA. Atomic force microscopy can be used to mechanically stimulate osteoblasts and evaluate cellular strain distributions. Ultramicroscopy. 2001; 86:85–95. [PubMed: 11215637]

Chen Q, Xiao P, Chen J, Cai J, Cai X, Ding H, Pan Y. AFM studies of cellular mechanics during osteogenic differentiation of human amniotic fluid-derived stem cells. Analytical Sciences. 2010; 26:1033–1037. [PubMed: 20953044]

Collinsworth AM, Zhang S, Kraus WE, Truskey GA. Apparent elastic modulus and hysteresis of skeletal muscle cells throughout differentiation. American Journal of Physiology-Cell Physiology. 2002; 283:C1219–C1227. [PubMed: 12225985]

Costa KD. Single-cell elastography: probing for disease with the atomic force microscope. Disease Markers. 2003; 19:139–154. [PubMed: 15096710]

Costa, KD. Imaging and probing cell mechanical properties with the atomic force microscope. In: Taatjes, DJMBT., editor. Methods in Molecular Medicine. 2006. p. 331-361.

Costa KD, Sim AJ, Yin FCP. Non-Hertzian approach to analyzing mechanical properties of endothelial cells probed by atomic force microscopy. Journal of Biomechanical Engineering. 2006; 128:176–184. [PubMed: 16524328]

Cross SE, Yu-Sheng J, Jianyu R, Gimzewski JK. Nanomechanical analysis of cells from cancer patients. Nature Nanotechnology. 2007; 2:780–783.

Darling E, Zauscher S, Guilak F. Viscoelastic properties of zonal articular chondrocytes measured by atomic force microscopy. Osteoarthritis and Cartilage. 2006; 14:571–579. [PubMed: 16478668]

Darling EM, Topel M, Zauscher S, Vail TP, Guilak F. Viscoelastic properties of human mesenchymally-derived stem cells and primary osteoblasts, chondrocytes, and adipocytes. Journal of Biomechanics. 2008; 41:454–464. [PubMed: 17825308]

Darling EM, Zauscher S, Block JA, Guilak F. A thin-layer model for viscoelastic, stress-relaxation testing of cells using atomic force microscopy: do cell properties reflect metastatic potential? Biophysical Journal. 2007; 92:1784–1791. [PubMed: 17158567]

Favre M, Polesel-Maris J, Overstolz T, Niedermann P, Dasen S, Gruener G, Ischer R, Vettiger P, Liley M, Heinzelmann H, Meister A. Parallel AFM imaging and force spectroscopy using two-dimensional probe arrays for applications in cell biology. Journal of Molecular Recognition. 2011; 24:446–452. [PubMed: 21504022]

Fung CKM, Seiffert-Sinha K, Lai KWC, Yang R, Panyard D, Zhang J, Xi N, Sinha AA. Investigation of human keratinocyte cell adhesion using atomic force microscopy. Nanomedicine: Nanotechnology, Biology and Medicine. 2010; 6:191–200.

Goldsbury, CS.; Scheuring, S.; Kreplak, L. Introduction to atomic force microscopy (AFM) in biology. In: Coligan John, E.; Dunn Ben, M.; Speicher David, W.; Wingfield Paul, T.; Ploegh Hidde, L.; Gwen, Taylor, editors. Current Protocolsin Protein Science. John Wiley & Sons, Inc; 2001.

Haga H, Sasaki S, Kawabata K, Ito E, Ushiki T, Sambongi T. Elasticity mapping of living fibroblasts by AFM and immunofluorescence observation of the cytoskeleton. Ultramicroscopy. 2000; 82:253–258. [PubMed: 10741677]

Hertz H. Ueber die Berührung fester elastischer Körper. Journal Für die Reine und Angewandte Mathematik (Crelle's Journal). 1882; 1882:156–171.

Jayasuriya AC, Bhat A. Mesenchymal stem cell function on hybrid organic/inorganic microparticles in vitro. Journal of Tissue Engineering and Regenerative Medicine. 2010; 4:340–348. [PubMed: 20033925]

Jena, BP.; Hörber, JKH. Atomic Force Microscopy in Cell Biology. Academic Press; California, USA: 2002.

Joo S, Ko IK, Atala A, Yoo JJ, Lee SJ. Amniotic fluid-derived stem cells in regenerative medicine research. Archives of Pharmacal Research. 2012; 35:271–280. [PubMed: 22370781]

Jung YG, Lawn BR, Martvniuk M, Han H, Xiao ZH. Evaluation of elastic modulus and hardness of thin films by nanoindentation. Journal of Materials Research. 2004; 19:3076–3080.

Kagiwada H, Nakamura C, Kihara T, Kamiishi H, Kawano K, Nakamura N, Miyake J. The mechanical properties of a cell, as determined by its actin cytoskeleton, are important for nanoneedle insertion into a living cell. Cytoskeleton. 2010; 67:496–503. [PubMed: 20535819]

Kelly GM, Kilpatrick JI, Van Es MH, Weafer PP, Prendergast PJ, Jarvis SP. Bone cell elasticity and morphology changes during the cell cycle. Journal of Biomechanics. 2011; 44:1484–1490. [PubMed: 21481877]

Kim J, Lee Y, Kim H, Hwang K, Kwon H, Kim S, Cho D, Kang S, You J. Human amniotic fluid-derived stem cells have characteristics of multipotent stem cells. Cell Proliferation. 2007; 40:75–90. [PubMed: 17227297]

Kirmizis D, Logothetidis S. Atomic force microscopy probing in the measurement of cell mechanics. International Journal of Nanomedicine. 2010; 5:137–145. [PubMed: 20463929]

Kolambkar YM, Peister A, Ekaputra AK, Hutmacher DW, Guldberg RE. Colonization and osteogenic differentiation of different stem cell sources on electrospun nanofiber meshes. Tissue Engineering Part A. 2010; 16:3219–3230. [PubMed: 20504075]

Lekka M. Atomic force microscopy: a tip for diagnosing cancer. Nature Nanotechnology. 2012; 7:691–692.

Lekka M, Pogoda K, Gostek J, Klymenko O, Prauzner-Bechcicki S, Wiltowska-Zuber J, Jaczewska J, Lekki J, Stachura Z. Cancer cell recognition–mechanical phenotype. Micron. 2012; 43:1259–1266. [PubMed: 22436422]

Lim C, Zhou E, Quek S. Mechanical models for living cells—a review. Journal of Biomechanics. 2006; 39:195–216. [PubMed: 16321622]

Mathur AB, Collinsworth AM, Reichert WM, Kraus WE, Truskey GA. Endothelial, cardiac muscle and skeletal muscle exhibit different viscous and elastic properties as determined by atomic force microscopy. Journal of Biomechanics. 2001; 34:1545–1553. [PubMed: 11716856]

Ng L, Hung HH, Sprunt A, Chubinskaya S, Ortiz C, Grodzinsky A. Nanomechanical properties of individual chondrocytes and their developing growth factor-stimulated pericellular matrix. Journal of Biomechanics. 2007; 40:1011–1023. [PubMed: 16793050]

Nikkhah M, Strobl JS, Schmelz EM, Agah M. Evaluation of the influence of growth medium composition on cell elasticity. Journal of Biomechanics. 2011; 44:762–766. [PubMed: 21109247]

Pogoda K, Jaczewska J, Wiltowska-Zuber J, Klymenko O, Zuber K, Fornal M, Lekka M. Depth-sensing analysis of cytoskeleton organization based on AFM data. European Biophysics Journal. 2012; 41:79–87. [PubMed: 22038077]

Qian L, Li M, Zhou Z, Yang H, Shi X. Comparison of nano-indentation hardness to microhardness. Surface and Coatings Technology. 2005; 195:264–271.

Quist, AP.; Lal, R. Characterization of nanoscale biological systems: multimodal atomic force microscopy for nanoimaging, nanomechanics, and biomolecular interactions. In: Gabriel, AS.; Vladimir, P., editors. Nanotechnology for Biology and Medicine at the Building Block Level. Springer; New York: 2012. p. 45-68.

Rodrigues MT, Lee BK, Lee SJ, Gomes ME, Reis RL, Atala A, Yoo JJ. The effect of differentiation stage of amniotic fluid stem cells on bone regeneration. Biomaterials. 2012a; 33:6069–6078. [PubMed: 22672834]

Rodrigues MT, Lee SJ, Gomes ME, Reis RL, Atala A, Yoo JJ. Amniotic fluid-derived stem cells as a cell source for bone tissue engineering. Tissue Engineering Part A. 2012b; 18:2518–2527. [PubMed: 22891759]

Rotsch C, Radmacher M. Drug-induced changes of cytoskeletal structure and mechanics in fibroblasts: an atomic force microscopy study. Biophysical Journal. 2000; 78:520–535. [PubMed: 10620315]

Ruiz JP, Pelaez D, Dias J, Ziebarth NM, Cheung HS. The effect of nicotine on the mechanical properties of mesenchymal stem cells. Cell Health and Cytoskeleton. 2012; 4:29–35. [PubMed: 23060733]

Sen S, Subramanian S, Discher DE. Indentation and adhesive probing of a cell membrane with AFM: theoretical model and experiments. Biophysical Journal. 2005; 89:3203–3213. [PubMed: 16113121]

Siegel N, Rosner M, Hanneder M, Freilinger A, Hengstschläger M. Human amniotic fluid stem cells: a new perspective. Amino Acids. 2008; 35:291–293. [PubMed: 17710362]

Siegel N, Rosner M, Hanneder M, Valli A, Hengstschläger M. Stem cells in amniotic fluid as new tools to study human genetic diseases. Stem Cell Reviews and Reports. 2007; 3:256–264. [PubMed: 17955390]

Simon A, Cohen-Bouhacina T, Aime JP, Porte MC, Amedee J, Baquey C. Heterogeneous cell mechanical properties: an atomic force microscopy study. Cellular and Molecular Biology. 2004; 50:255–266. [PubMed: 15209346]

Simon A, Cohen-Bouhacina T, Porte MC, Aime JP, Amedee J, Bareille R, Baquey C. Characterization of dynamic cellular adhesion of osteoblasts using atomic force microscopy. Cytometry A. 2003; 54:36–47. [PubMed: 12820119]

Simon A, Durrieu MC. Strategies and results of atomic force microscopy in the study of cellular adhesion. Micron. 2006; 37:1–13. [PubMed: 16171998]

Sirghi L, Ponti J, Broggi F, Rossi F. Probing elasticity and adhesion of live cells by atomic force microscopy indentation. European Biophysics Journal. 2008; 37:935–945. [PubMed: 18365186]

Skardal A, Mack D, Atala A, Soker S. Substrate elasticity controls cell proliferation, surface marker expression and motile phenotype in amniotic fluid-derived stem cells. Journal of the Mechanical Behavior of Biomedical Materials. 2012; 17:307–316. [PubMed: 23122714]

Sneddon IN. The relation between load and penetration in the axisymmetric boussinesq problem for a punch of arbitrary profile. International Journal of Engineering Science. 1965; 3:47–57.

Suresh S. Mechanical response of human red blood cells in health and disease: some structure-property-function relationships. Journal of Materials Research. 2006; 21:1871–1877.

Svaldo Lanero T, Cavalleri O, Krol S, Rolandi R, Gliozzi A. Mechanical properties of single living cells encapsulated in polyelectrolyte matrixes. Journal of Biotechnology. 2006; 124:723–731. [PubMed: 16600412]

Takai E, Costa KD, Shaheen A, Hung CT, Guo XE. Osteoblast elastic modulus measured by atomic force microscopy is substrate dependent. Annals of Biomedical Engineering. 2005; 33:963–971. [PubMed: 16060537]

Titushkin I, Cho M. Modulation of cellular mechanics during osteogenic differentiation of human mesenchymal stem cells. Biophysical Journal. 2007; 93:3693–3702. [PubMed: 17675345]

Vié V, Giocondi MC, Lesniewska E, Finot E, Goudonnet JP, Le Grimellec C. Tapping-mode atomic force microscopy on intact cells: optimal adjustment of tapping conditions by using the deflection signal. Ultramicroscopy. 2000; 82:279–288. [PubMed: 10741680]

Weisenhorn AL, Khorsandi M, Kasas S, Gotzos V, Butt HJ. Deformation and height anomaly of soft surfaces studied with an AFM. Nanotechnology. 1993; 4:106–113.

Wu, X.; Sun, Z.; Meininger, GA.; Muthuchamy, M. Application of Atomic Force Microscopy Measurements on Cardiovascular Cells Cardiovascular Development. Peng, X.; Antonyak, M., editors. Humana Press; York, NY, USA: 2012. p. 229-244.

Yourek G, Hussain MA, Mao JJ. Cytoskeletal changes of mesenchymal stem cells during differentiation. ASAIO Journal. 2007; 53:219–228. [PubMed: 17413564]

Zhu Y, Dong Z, Wejinya UC, Jin S, Ye K. Determination of mechanical properties of soft tissue scaffolds by atomic force microscopy nanoindentation. Journal of Biomechanics. 2011; 44:2356–2361. [PubMed: 21794867]

Zitzler L, Herminghaus S, Mugele F. Capillary forces in tapping mode atomic force microscopy. Physical Review B. 2002; 66:155436.

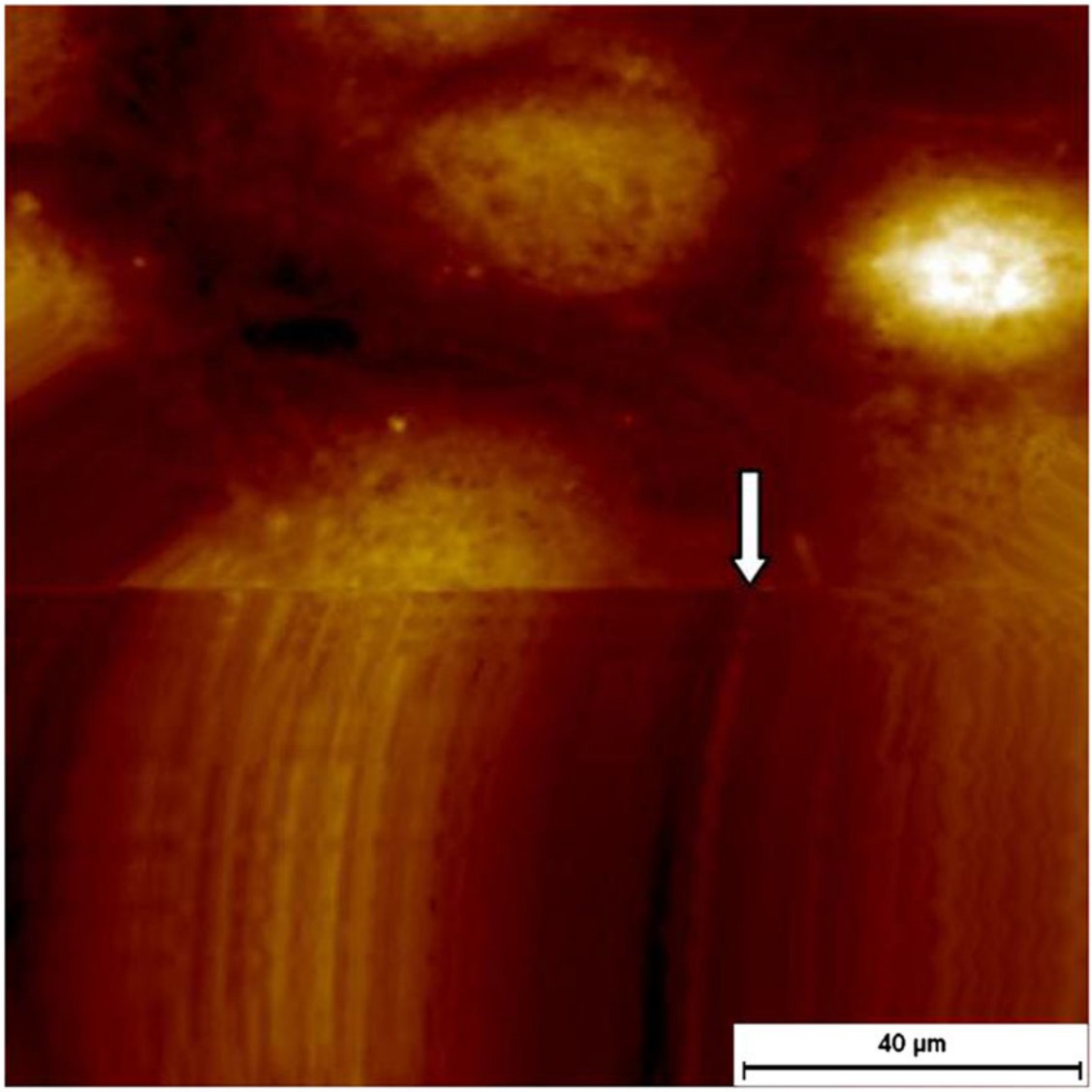

Fig. 1.
Detachment of OB6 cells observed during imaging with AFM contact mode. The arrow shows cell detachment line induced by the tip motion.

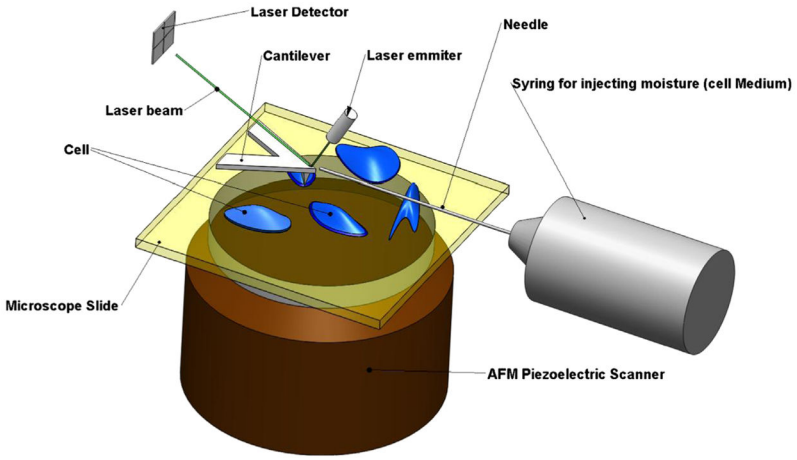

Fig. 2.

Test setup configuration for AFM imaging and indentation. During the imaging and indentation, the moisture was injected to the surface.

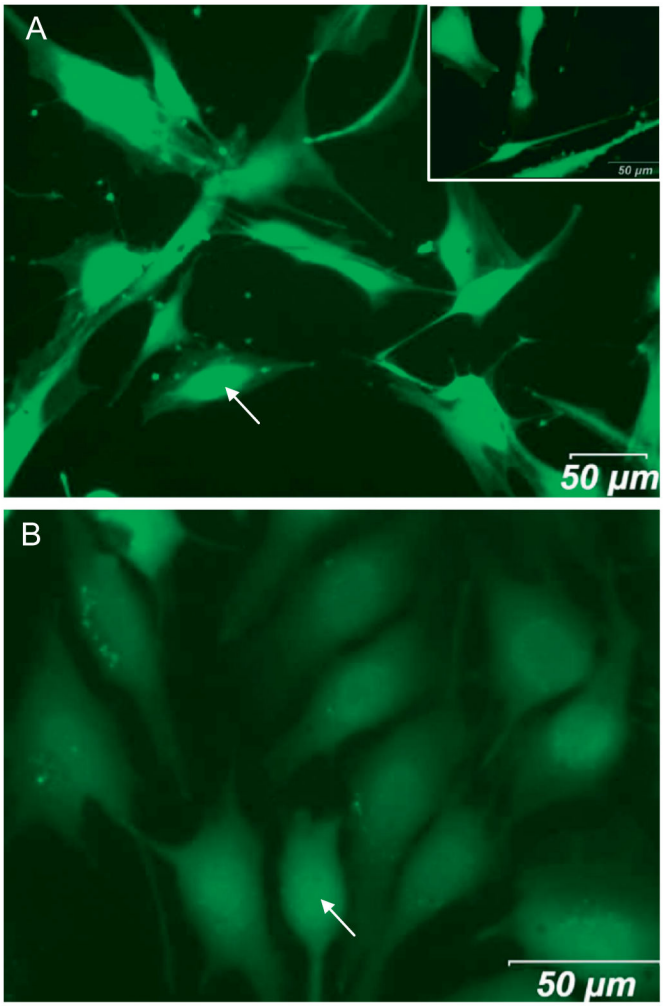

Fig. 3.

(A) Morphology of hAFS cells, (B) OB6 cells, treated with LIVE/DEAD cell assay. Arrows show the cell nuclei. Different parts of cells such as filaments, microtubes and nucleus are visible. (For interpretation of the references to color in this figure, the reader is referred to the web version of this article.)

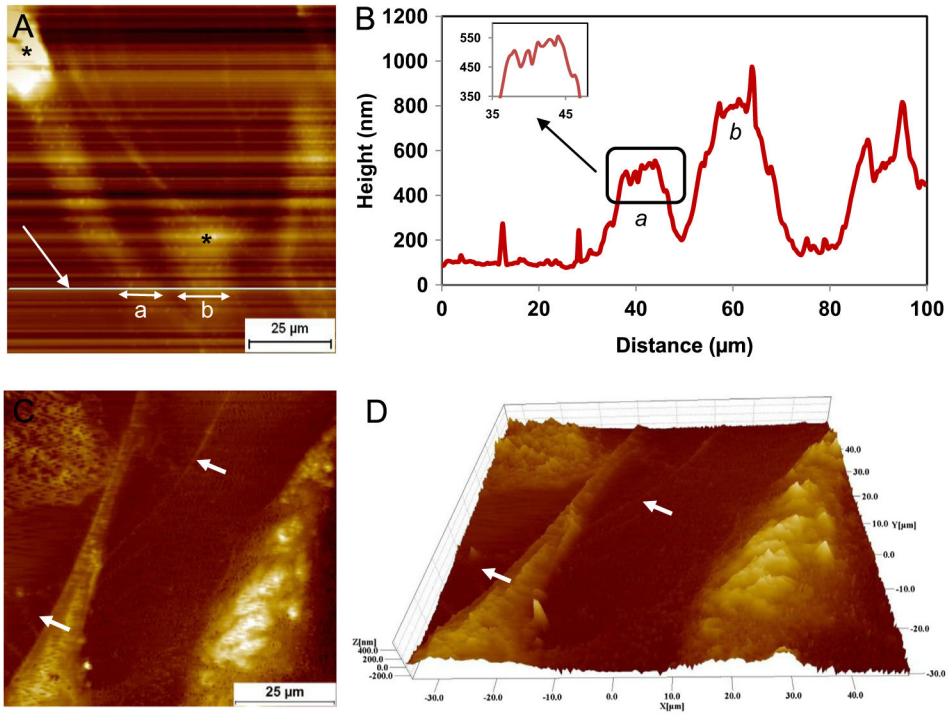

Fig. 4.

(A) Structural morphology of hAFS cells plated upon glass slides after 36 h, (B) height profile of the cell cytoskeleton throughout the indicated line, (C) cytoskeleton structure of hAFS cell, and (D) 3D image of hAFS cell. In the last two figures, the discrete actin filaments are shown by arrows.

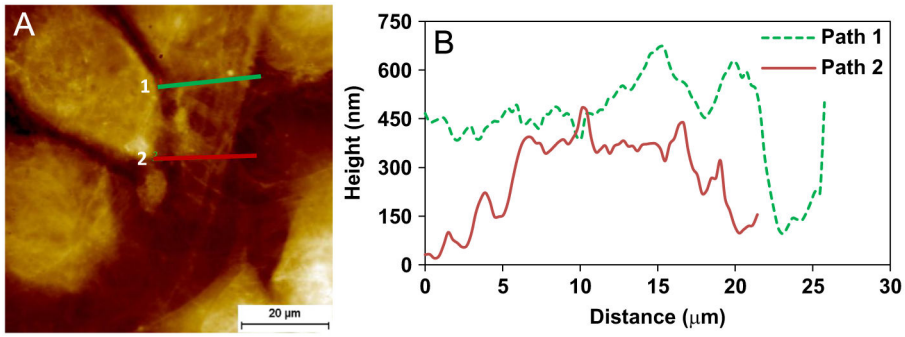

Fig. 5.

(A) Structural morphology of OB6 cells plated on glass slides after 36 h and (B) height profile of cell cytoskeleton along the two indicated path lines.

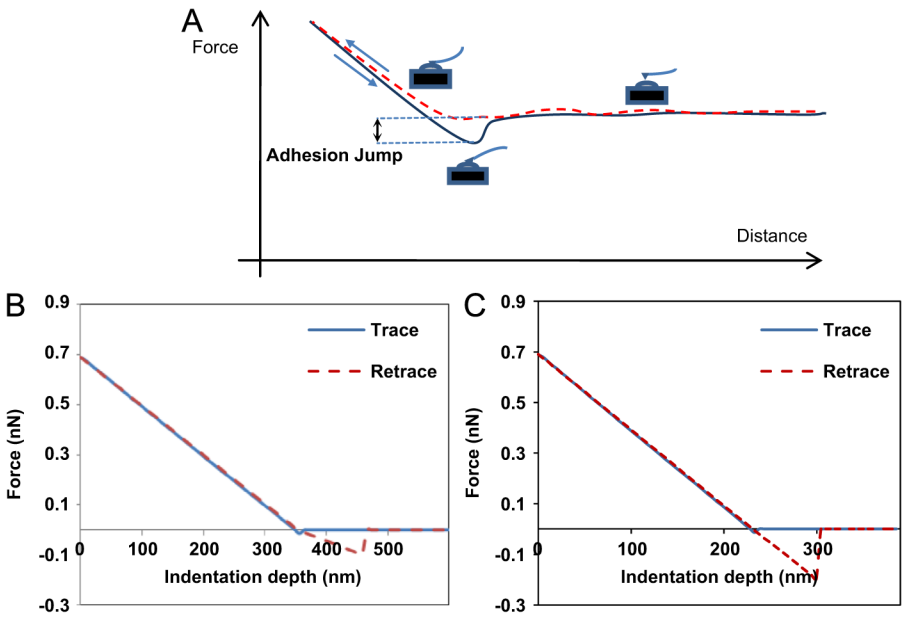

Fig. 6.

(A) Schematic figure of force–indentation curve, typical force–indentation curve for (B) hAFS cell, and (C) OB6 cell.

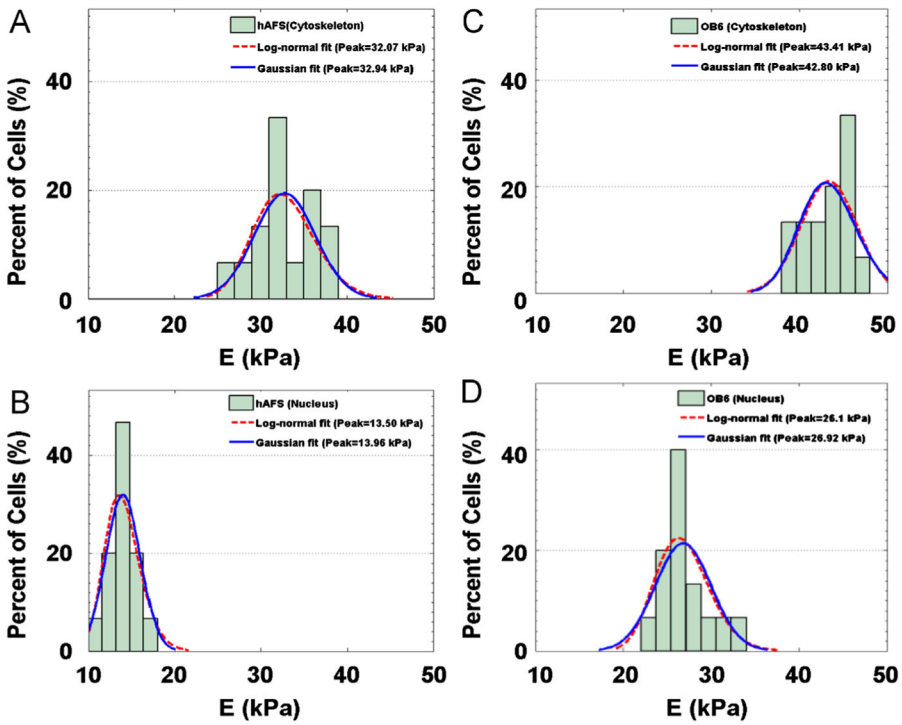

Fig. 7.

Young's modulus distribution of hAFS cells (A) at cytoskeleton region, (B) at nucleus region, and for OB6 cells (C) at cytoskeleton region, and (D) at nucleus region.